Characterization of the homogeneous tissue mixture approximation in breast imaging dosimetry

Ioannis Sechopoulos[a)]
Department of Radiology and Imaging Sciences and Winship Cancer Institute, Emory University School of Medicine, 1701 Upper Gate Drive Northeast, Suite 5018, Atlanta, Georgia 30322

Kristina Bliznakova
Department of Medical Physics, University of Patras School of Health Sciences, 26500 Rio-Patras, Greece

Xulei Qin
Department of Radiology and Imaging Sciences, Emory University School of Medicine, 1701 Upper Gate Drive Northeast, Suite 5018, Atlanta, Georgia 30322

Baowei Fei and Steve Si Jia Feng
Department of Radiology and Imaging Sciences, Emory University School of Medicine, 1701 Upper Gate Drive Northeast, Suite 5018, Atlanta, Georgia 30322 and Department of Biomedical Engineering, Emory University and Georgia Institute of Technology, Atlanta, Georgia 30322

Purpose: To compare the estimate of normalized glandular dose in mammography and breast CT imaging obtained using the actual glandular tissue distribution in the breast to that obtained using the homogeneous tissue mixture approximation.

Methods: Twenty volumetric images of patient breasts were acquired with a dedicated breast CT prototype system and the voxels in the breast CT images were automatically classified into skin, adipose, and glandular tissue. The breasts in the classified images underwent simulated mechanical compression to mimic the conditions present during mammographic acquisition. The compressed thickness for each breast was set to that achieved during each patient's last screening cranio-caudal (CC) acquisition. The volumetric glandular density of each breast was computed using both the compressed and uncompressed classified images, and additional images were created in which all voxels representing adipose and glandular tissue were replaced by a homogeneous mixture of these two tissues in a proportion corresponding to each breast's volumetric glandular density. All four breast images (compressed and uncompressed; heterogeneous and homogeneous tissue) were input into Monte Carlo simulations to estimate the normalized glandular dose during mammography (compressed breasts) and dedicated breast CT (uncompressed breasts). For the mammography simulations the x-ray spectra used was that used during each patient's last screening CC acquisition. For the breast CT simulations, two x-ray spectra were used, corresponding to the x-ray spectra with the lowest and highest energies currently being used in dedicated breast CT prototype systems under clinical investigation. The resulting normalized glandular dose for the heterogeneous and homogeneous versions of each breast for each modality was compared.

Results: For mammography, the normalized glandular dose based on the homogeneous tissue approximation was, on average, 27% higher than that estimated using the true heterogeneous glandular tissue distribution (Wilcoxon Signed Rank Test $p = 0.00046$). For dedicated breast CT, the overestimation of normalized glandular dose was, on average, 8% (49 kVp spectrum, $p = 0.00045$) and 4% (80 kVp spectrum, $p = 0.000089$). Only two cases in mammography and two cases in dedicated breast CT with a tube voltage of 49 kVp resulted in lower dose estimates for the homogeneous tissue approximation compared to the heterogeneous tissue distribution.

Conclusions: The normalized glandular dose based on the homogeneous tissue mixture approximation results in a significant overestimation of dose to the imaged breast. This overestimation impacts the use of dose estimates in absolute terms, such as for risk estimates, and may impact some comparative studies, such as when modalities or techniques with different x-ray energies are used. The error introduced by the homogeneous tissue mixture approximation in higher energy x-ray modalities, such as dedicated breast CT, although statistically significant, may not be of clinical concern. Further work is required to better characterize this overestimation and potentially develop new metrics or correction factors to better estimate the true glandular dose to breasts undergoing imaging with ionizing radiation. © *2012 American Association of Physicists in Medicine.* [http://dx.doi.org/10.1118/1.4737025]

I. INTRODUCTION

A comprehensive understanding of the dosimetric characteristics of clinical imaging modalities involving ionizing radiation is of paramount importance. This is especially so for modalities which are used or which might be used as screening technologies. Probably the most well-established screening test involving ionizing radiation currently is mammography. As such, the radiation dosimetry characteristics of mammography have been studied extensively for at least five decades.[1–11] In 1979, Hammerstein *et al.*[2] proposed that the dose metric of interest in mammography should be the dose deposited in the glandular tissue portion of the breast, since this is the tissue at risk of breast cancer development. Given the variability of glandular tissue distribution in patients' breasts, Hammerstein *et al.* defined an "average" breast as being 6 cm thick, with a skin and adipose outer layer 0.5 cm deep and the interior composed of a homogeneous mixture of 50% adipose and 50% glandular tissue and defined the mean glandular dose as the dose to the glandular portion of this homogeneous tissue mixture. This gave rise to the common "50/50 breast" and the mean glandular dose metric used in subsequent mammography dosimetry studies[3–11] in addition to dosimetry studies of newly developed breast imaging modalities such as breast tomosynthesis and dedicated breast CT.[12–18] In many of these subsequent studies, investigators studied how the mean glandular dose varies for different proportions of glandular to adipose tissue in the homogeneous mixture, as well as for different breast thicknesses and sizes.

Since the definition of the "average" breast by Hammerstein *et al.*, new technology has allowed for a refinement of its definition. Yaffe *et al.* recently used dedicated breast CT (BCT) imaging data and a glandular density estimation algorithm to determine how dense an "average" breast actually is, finding that the mean glandular fraction is approximately 15%–20%, and that rarely is a 50% dense breast encountered clinically.[19] Another study based on BCT data has found that the mean breast skin thickness is approximately 1.45 mm, considerably less than that previously used in breast dose studies.[20]

However, it should be noted that Hammerstein *et al.* clarified that the mean glandular dose metric applied to a homogeneous breast could be used for "comparing doses delivered with different radiographic techniques," while "detailed information will have to be obtained on the amount and distribution of gland tissue in many individual cases" before individual risk estimates can be made.[2] Therefore, it is clear that the dose data of Hammerstein *et al.*, in addition to all subsequent data on mean glandular dose based on the homogeneous breast approximation, should only be used to compare acquisition techniques (e.g., different tube voltages), protocols (e.g., one view vs two views), technologies (e.g., screen-film vs digital), and modalities (e.g., mammography vs tomosynthesis), but not in absolute terms to estimate risk. However, since no better estimate of dose to the breast glandular tissue is available, mean glandular dose estimates from different sources[9,21–23] have repeatedly been used to estimate the risk associated with mammography and to provide guidance to physicians during discussions with patients about mammographic screening.[24–28] In addition, the use of the homogeneous breast approximation might also not be appropriate for comparative studies of certain characteristics, e.g., in which the x-ray energy used by two modalities being compared differs considerably (e.g., mammography vs BCT).

Given these issues, this study aims to investigate how appropriate using the homogeneous approximation actually is compared to the true mean dose to the glandular tissue. With the development of BCT, acquiring actual high resolution volumetric breast tissue distribution information *in vivo* is possible for the first time.

Recently, Yi *et al.*, using only four mastectomy specimens and a benchtop BCT system, performed a comparison of the mean dose to the entire breast (not only the glandular portion) estimated using either the actual breast tissue distribution of adipose and glandular tissue as obtained from BCT images of the specimens and the corresponding homogeneous tissue mixture approximation, finding no significant difference between these two groups.[29] However, as mentioned, that study compared the average breast dose, not the mean glandular dose, included only four mastectomy samples that lacked skin imaged with a benchtop BCT system and only compared the dose estimates for BCT imaging, and therefore used a high energy x-ray spectrum (tube voltage of 80 kVp with a first half value layer of 4.08 mm Al).[29] In another study, Dance *et al.* compared the normalized mean glandular dose to heterogeneous, structured computer simulated phantoms undergoing mammography to previously published values for homogeneous breast phantoms of equivalent glandular density and compressed breast thickness.[30] In that study, the structured phantoms ranged from a thickness of 40 mm to 80 mm and a glandular density of 25%–100%. In addition, all mammography acquisitions were simulated as performed with a single spectrum (Mo/Mo 28 kVp). The authors found that the normalized mean glandular dose was overestimated by the homogeneous simple phantom by 10%–43%. Subsequently, Dance *et al.* modified the structured phantom to deform the glandular structures inside the breast so that they could be closer or further away from the breast skin layer and studied what impact these deformations had on the comparison of normalized mean glandular dose estimates. Although that study provided some indication that the homogeneous breast tissue mixture approximation results in an overestimate of the normalized mean glandular dose compared to a structured breast tissue composition, no comparison to actual patient breast tissue distributions was made, and, as mentioned, the acquisition conditions studied were limited to mammography with a single spectrum.

In this study, using 20 patient BCT images acquired *in vivo* with a BCT clinical prototype, the normalized mean dose to the actual glandular tissue was estimated and compared to that of the homogeneous approximations of these breasts, both for BCT and mammography acquisitions. With this initial study, we aim to determine if there is a substantial difference between the actual mean glandular dose and the mean glandular dose to the homogenous approximation of the breast for both imaging modalities. If so, a larger study with a large number
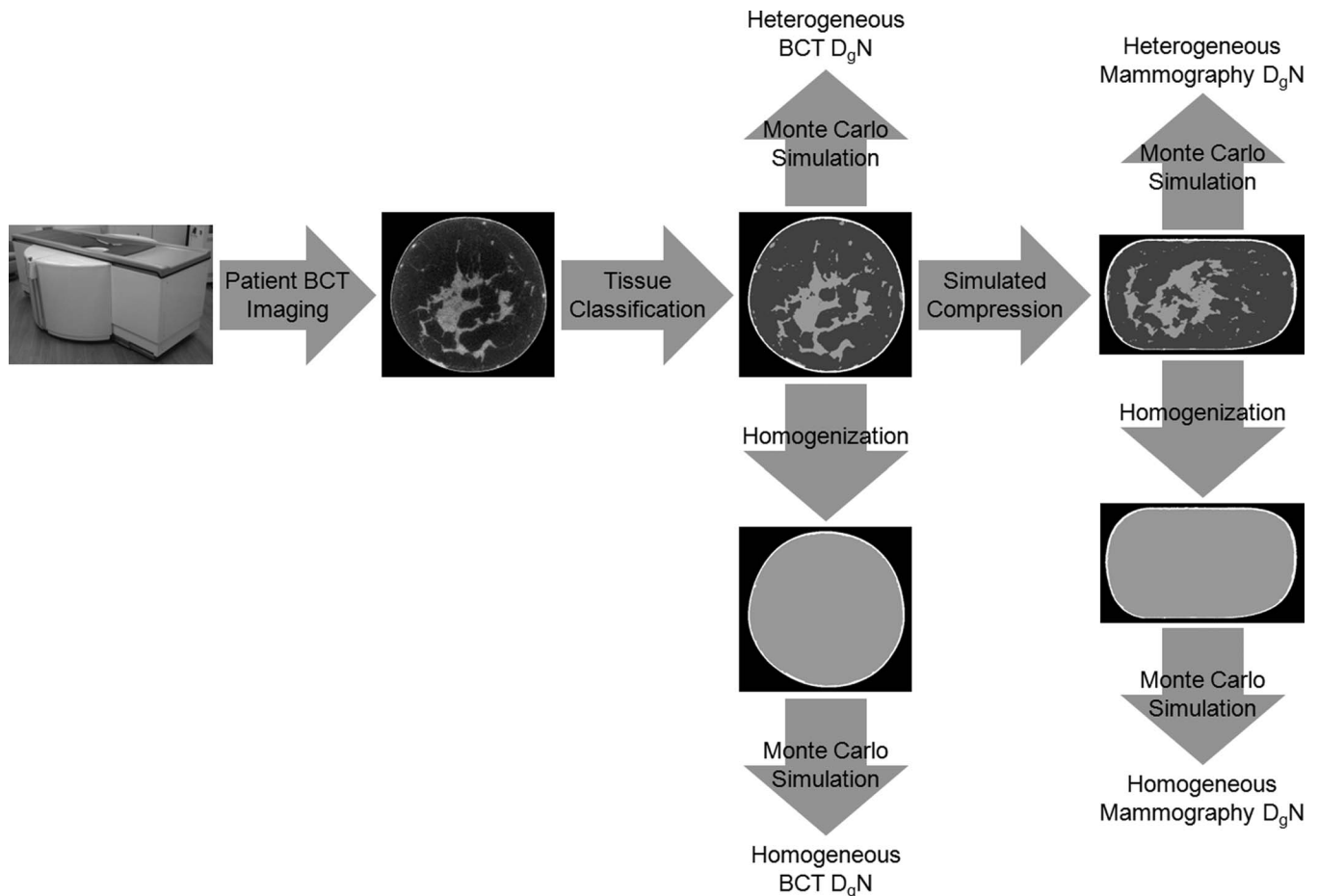
FIG. 1. Diagram of the process followed in this study. The normalized glandular dose (D_gN) resulting from the heterogeneous and homogeneous definitions of the patient breasts was compared for both mammography and BCT. The Monte Carlo simulations of BCT imaging included both 49 kVp and 80 kVp x-ray spectra.

of patient images would be needed to attempt to characterize how this difference varies with breast dimension and composition and imaging conditions, and ultimately, attempt to determine relevant adjustment factors or novel metrics that could result in better estimates of actual mean glandular dose that could be used in absolute terms for risk estimates.

II. METHODS AND MATERIALS

To estimate the mean dose to the actual glandular tissue in heterogeneous volumetric breast images and to the glandular tissue component of the homogeneous breast tissue mixture approximation, the process shown in Fig. 1 was followed, for which details are provided below.

II.A. Dedicated breast computed tomography acquisitions

The BCT images for all 20 patients were acquired for on-going IRB-approved clinical studies after informed consent was obtained from the patients. As part of the consent, the patients released these images for use in other research projects after anonymization.

All BCT images were acquired with a dedicated BCT clinical prototype (Koning Corp., West Henrietta, NY) installed at our institution. The details of this imaging system have been previously published,[31–34] so only the most relevant details to this study will be mentioned here. During acquisition of a BCT scan, the patient lies prone on the system table with the breast being imaged pendant through an opening on the table. The breast remains uncompressed during the imaging, which involves acquisition of 300 projections about a complete revolution of the x-ray source and flat-panel detector in 10 s. The BCT system uses an x-ray spectrum produced by a tungsten target with a tube voltage of 49 kVp filtered by an added aluminum filter, resulting in a first half value layer of 1.39 mm Al.[17] The system's reconstruction algorithm, based on the FDK reconstruction,[35] results in volumetric images with cubic voxels 0.273 mm in size.

II.B. Tissue classification

The voxels in the reconstructed BCT images were automatically classified into four categories: air, skin, adipose, and glandular tissue. For this, a previously described and validated algorithm was used which consists of four major steps: (i) bias correction to reduce the cupping artifact in BCT; (ii) noise filtering using a multiscale bilateral filter; (iii) adipose and glandular tissue classification using a modified fuzzy

C-means classification method; and (iv) skin tissue classification using a morphologic method.[36]

Cupping artifacts, which reduce voxel value accuracy,[37] introduce a variation in the voxel value for the same tissue depending on its location in the breast, making accurate classification challenging if not corrected first. Cupping occurs due to a variation in the x-ray scatter signal included in the BCT projections throughout the projection of the breast[38,39] and due to beam hardening.[40] In the method used here, the cupping artifact is corrected using a nonparametric coarse-to-fine approach with an entropy-related cost function to improve reliability in the automated correction. To decrease image noise prior to classification, a multiscale filter introduced by Tomasi[41] was used, as described previously.[36] Tissue classification into adipose and glandular voxels was performed using a modified fuzzy C-means algorithm, which iteratively performs an optimal partition of the image by minimizing a weighted objective function. By allowing for fuzzy partitioning, each voxel is assigned a probability of belonging to each of the two groups being classified, and the final classification is made by assigning the voxel to the group for which that voxel has the highest probability of membership. Finally, skin voxels were identified using morphologic operations to assign the outer voxels of the breast as skin tissue.

From the classified images the total mass of the glandular and adipose tissue included in the BCT images of each patient breast was computed by counting the number of voxels classified as glandular or adipose tissue and multiplying this number by the voxel size $(0.273 \text{ mm})^3$ and the corresponding tissue density (adipose: 0.93 g/cm^3 and glandular: 1.04 g/cm^3).[2] The ratio of the total glandular mass to the sum of both masses was used as the volumetric breast glandular density for the breasts undergoing BCT acquisition.

II.C. Mechanical compression simulation

A simulation of mechanical compression during mammographic acquisition was applied to the breasts in the classified volumetric BCT images using a previously described method based on a linear spring model.[42] In summary, in this method, the classified breast is divided into "model elements" each comprising 27 voxels. These model elements are connected to each other with springs which are assumed to have a linear and isotropic modulus of elasticity. Tissue incompressibility (constant total volume) is imposed by defining variable equilibrium lengths for the springs. To allow for the compression simulation to be performed in a reasonable time frame, the method described by Zyganitidis *et al.* was implemented to run in multithreaded parallel form, using the Message Passing Interface for interprocessor communication implemented through mpich2.[56] The modulus of elasticity of the skin, adipose, and glandular tissue was set to 88.0, 1.0, and 10.0 kPa, respectively.[43]

The degree of compression used in the simulations was such that the final compressed breast thickness matched that recorded for each patient's latest cranio-caudal (CC) view screening mammogram. Most, but not all, of the breast tissue included in the BCT images was simulated as being placed
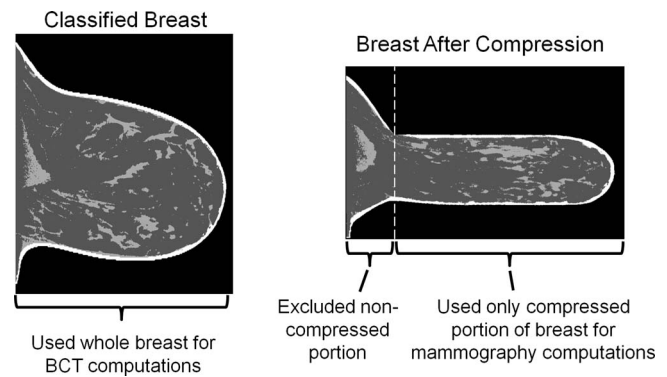

FIG. 2. Sagittal BCT slice of a classified patient breast before and after tissue classification. The whole classified uncompressed breast was used to compute the volumetric glandular density in BCT and for the Monte Carlo simulations to estimate D_gN in BCT. However, only the compressed portion of the breast was used to compute the volumetric glandular density in the mammography cases and for the mammography Monte Carlo simulations. For this breast, the volumetric glandular density based on the BCT case was 12.7% and in the mammography case was 15.2%.

between the breast support plate and the breast compression plate and, therefore, was simulated as undergoing compression. To compress as much breast tissue as possible, it was assumed that the patients' chest wall was located immediately posterior to the breast tissue included in the BCT image. The edges of the compression and support plates were placed as close as possible to the chest wall, leaving, for the majority of the breasts, up to 2 mm of uncompressed tissue. For the largest breasts, however, placing the edges of the plates that close to the chest wall and achieving the desired compression thickness would have resulted in about a 70% compression, which is not a realistic compression level. Therefore, for these cases, as shown as an example in Fig. 2, the edges of the plates were positioned approximately 2 cm away from the chest wall.

Since the uncompressed portion of the breast tissue was excluded from the mammographic simulation, the breast glandular density of only the compressed portion of the breast was computed using the same method described above for the BCT volumetric breast density. This density was denoted the volumetric breast density for the mammographic acquisition (Fig. 2). By estimating the volumetric breast density for each modality, a more accurate comparison between the heterogeneous and homogeneous tissue dose estimates in each modality was ensured.

II.D. Monte Carlo simulations

Previously described Monte Carlo simulations of mammography and tomosynthesis[15,44] and BCT (Ref. 17) based on the Geant4 toolkit (version 9.4) (Refs. 45 and 46) were modified to use voxelized volumes as models of the breast as opposed to simple geometric volumes.

The mammography simulation consisted of an isotropic x-ray point source emitting x-rays only towards a 24 cm × 29 cm detector located 70 cm away. The air gap between detector and breast volume was 2.5 cm, and the breast support plate and compression plate were included in the simulations.

The voxelized compressed breast volume was placed at the center of the x-ray beam and detector in the chest wall direction, with the chest wall edge of the breast at the central ray, as is common in mammography geometries. As shown in Fig. 2, the uncompressed portion of the voxelized breast volume was excluded from the simulation. To include the effect of backscatter from the rest of the body, a large cuboid of water was simulated as the body. The x-ray source was modeled as emitting a spectrum of x-rays, with the probability density functions defined using the spectral models published by Boone *et al.*[47] The spectrum used for each simulation was varied to match the target/filter combination and tube voltage setting used for each patient's latest CC view screening mammogram. For each breast, a single acquisition of a mammographic view was simulated.

The BCT simulation consisted of an isotropic x-ray point source which emitted x-rays towards a 29.8 cm × 39.7 cm detector located 92.3 cm away. The center of the voxelized breast volume was located at the isocenter of the simulated system, 27.3 cm away from the detector, with the chest wall edge of the voxelized volume at the central ray, as is common in current BCT system geometries. Again, the rest of the body was simulated as a large cuboid of water. The simulations of the BCT acquisitions were performed with x-ray spectra modeled as produced with a tungsten target and both an aluminum filter and a tube voltage of 49 kVp (first HVL = 1.39 mm Al) (Ref. 48) and a copper and a tube voltage of 80 kVp (first HVL = 5.697 mm Al).[47] These two spectra represent two of the three spectra used by BCT clinical prototypes currently being used for clinical studies.[34,49,50] These two spectra were chosen since these encompass the extremes of the x-ray beam quality of the three spectra currently being used (third spectrum: 60 kVp, 0.51 mm Ce filter, first HVL = 2.95 mm Al).[51] For each breast, 36 BCT projection acquisitions were simulated, each varying the position of the x-ray source and detector to simulate different projection angles, ranging from 0° to 350°, in 10° steps. The normalized dose results from the 36 projections were averaged to estimate the normalized dose for a complete BCT acquisition.

For each acquisition simulation of both mammography and BCT, 10^6 x-rays were simulated as emitted from the x-ray source and were followed until they were completely absorbed or left the simulation volume. This number of x-rays was enough to obtain an uncertainty level of the total energy deposited in the voxels being measured below 1%, which was estimated for each simulation using the algorithm described by Sempau *et al.*[52]

For the first set of simulations, the voxelized volumes representing patient breasts, both compressed and uncompressed, were input into the mammography and BCT simulations, respectively, with the voxels in the volumes marked as denoting air, breast skin tissue, breast glandular tissue, or breast adipose tissue. The composition of the breast tissues was defined using the description in Hammerstein *et al.*[2] Each energy deposition event that occurred in the breast voxels marked as representing glandular tissue was recorded. From the total energy deposition to all the glandular tissue voxels the mean dose to the glandular tissue was computed and normalized

by the skin entrance (mammography) and isocenter with no breast present (BCT) air kerma. Therefore, the normalized glandular dose for the heterogeneous simulations was determined using the equation

$$D_g N_{\text{heterogeneous}} = \frac{\sum_n E_{\text{dep}}}{vm_g \sum_e \Phi(e)\Theta(e)}, \tag{1}$$

where E_{dep} is the energy deposited in all the voxels representing glandular tissue by each of the n x-rays simulated, v and m_g are the total number and mass of the glandular tissue voxels, respectively, and $\Phi(e)$ and $\Theta(e)$ are the reference x-ray fluence and fluence to air kerma conversion factor for x-ray energy e, respectively.

For the second set of simulations, the voxels representing adipose and glandular tissue were replaced with voxels representing a homogeneous mixture of these two materials, in the fraction corresponding to the volumetric breast glandular density computed for each modality as described above. For these simulations, the mean glandular dose was estimated by weighing each energy deposition event in these voxels by the ratio of the mass energy absorption coefficients (G), as described by Boone and Wilkinson and Heggie.[8,53] Again, the mean glandular dose estimate was normalized by the skin entrance (mammography) and isocenter with no breast present (BCT) air kerma. Therefore, the normalized glandular dose for the homogeneous simulations was determined using the following equations:

$$D_g N_{\text{homogeneous}} = \frac{\sum_n E_{\text{dep}} G(g, e)}{gm_t \sum_e \Phi(e)\Theta(e)} \tag{2}$$

and

$$G(g, e) = \frac{g\left(\frac{\mu_{\text{en}}}{\rho}\right)_g}{g\left(\frac{\mu_{\text{en}}}{\rho}\right)_g + (1 - g)\left(\frac{\mu_{\text{en}}}{\rho}\right)_a}, \quad \text{(Ref. 8)} \tag{3}$$

where g is the glandular density, m_t is the total mass of the breast tissue excluding skin [note that vm_g from Eq. (1) is equal to gm_t from Eq. (2)], $(\frac{\mu_{\text{en}}}{\rho})_g$ and $(\frac{\mu_{\text{en}}}{\rho})_a$ are the mass energy absorption coefficients of glandular and adipose tissue, respectively. The rest of the terms in these two equations are the same as those in Eq. (1).

For a single case, the heterogeneous and homogeneous voxelized volumes were binned by 4 × 4 × 4 to create versions with a lower spatial resolution. Monte Carlo simulations of the mammography and BCT acquisitions using these smaller volumes were again performed, but this time the energy depositions in the glandular tissue were tracked voxel-by-voxel, resulting in 3D maps of dose deposition. Again, for the BCT acquisitions a total of 36 projections were simulated. In this way, the distribution of the dose deposition could be compared. For these simulations, the voxels were binned to reduce the simulation to a reasonable time.

II.E. Heterogeneous vs homogeneous mean normalized glandular dose comparison

The normalized mean glandular dose in the heterogeneous breast simulations was compared to the corresponding homogeneous breast approximations for each modality and, in the case of BCT, for each of the two spectra simulated. Each set of paired results was statistically tested for a significant difference using the Wilcoxon Signed Rank test (SPSS Statistics 20.0, International Business Machines Corp., Armonk, NY).

II.F. Monte Carlo simulation validation

Although most portions of the Monte Carlo simulations used for this study have been previously validated,[15,17] the use of the breasts defined as voxelized volumes instead of simple geometric shapes needed to be validated. For this, the empirical measurements of the exposure in the five insert locations of a 16 cm diameter adult head CT phantom undergoing BCT acquisition previously published were simulated.[17] To perform this validation, a voxelized representation of the head CT phantom with 0.2 mm voxel sizes was generated and input into the BCT Monte Carlo simulation. The acquisition of a single projection and of a complete BCT acquisition (300 projections) was simulated and the results statistically compared to the empirical results using commercial software (TableCurve 2D 5.01.03, Systat Software Inc., Chicago IL and SPSS Statistics 20.0, International Business Machines Corp., Armonk, NY). Validation of this BCT setup was considered sufficient since the mammography simulation only differs from the former in details of the acquisition geometry (relative position of x-ray source, breast, and detector and size of detector) and x-ray energy.

II.G. Comparison to previous studies

The normalized glandular dose values obtained for the homogeneous breast tissue mixture approximation were compared to previously published values to obtain a secondary, approximate validation of our results. As is usual for breast dosimetry studies, the values from the comparison studies were estimated using regularly shaped breast phantoms of varying size and glandular density, so a considerable error in the comparison was expected. For comparison of the mammography normalized glandular dose, the values reported by Dance *et al.*[54] for the closest possible breast thickness, glandular density, and HVL and matching target/filter combination for each breast was computed using Tables II, III, and VI of that study. For BCT with a tube voltage of 49 kVp, the same procedure was used, using the values from Table I of Sechopoulos *et al.*,[17] for the closest chest wall to nipple distance and glandular density, with the equivalent diameter at the chest wall estimated to result in a breast of the closest total volume possible. Finally, for BCT with a tube voltage of 80 kVp, the range of normalized glandular dose for 0%–50% glandular density for a breast diameter of 10 cm at a tube voltage of 80 kVp was estimated from Fig. XIII(b) of Boone *et al.*[16]

TABLE I. Characteristics of the breast images included in study.

		Mammography	Breast CT
Number of cases		19	20
Glandular density	Mean (%)	24.0%	19.2%
	Range (%)	6.7%–54.3%	4.7%–42.7%
Difference in glandular density, BCT − Mammo	Mean (%)	−4.1%	
	Range (%)	−16.4% to −0.3%	
Compressed thickness	Mean (mm)	58.6	–
	Range (mm)	27–78	–

III. RESULTS

III.A. Monte Carlo simulation validation

The empirical and Monte Carlo results of the relative variation in exposure at the five insert locations of the head CT phantom normalized to that of the center position is shown in Fig. 3. As can be seen from the points and from the linear fits, there is excellent correspondence between the empirical and simulated data, both for the single projection distribution and for the complete BCT acquisition simulation. For both fits, the 95% confidence intervals for the fit coefficients for the offsets include zero and for the slopes include unity. Furthermore, for both the single projection and the complete BCT acquisition the simulation results were not significantly different from the measurements (Wilcoxon signed-rank test, $p = 0.593$ and $p = 0.068$, respectively).

III.B. Tissue classification and mechanical compression simulation

Of the 20 BCT images acquired, the mammographic screening data (compressed breast thickness and acquisition technique) for one case was not available. Therefore, all BCT
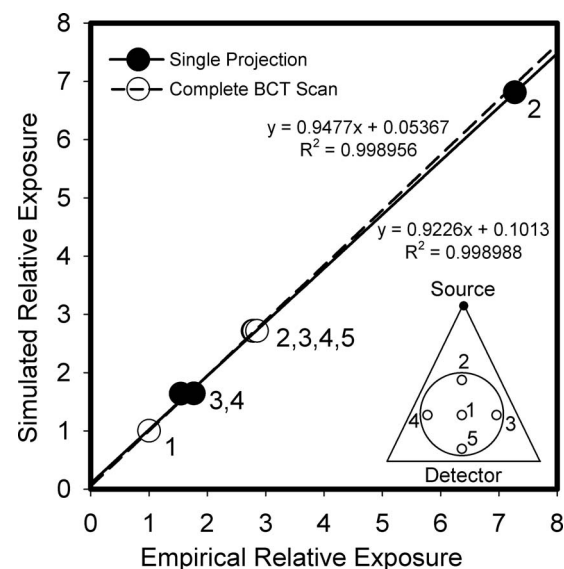

FIG. 3. Comparison of the Monte Carlo results to the empirical results for the validation of the simulations using voxelized volumes. As can be seen, good agreement was found between the simulations and the measurements.

TABLE II. Comparison of mean (range) of normalized glandular dose (in mGy/mGy air kerma) estimated for the homogeneous breast tissue mixture approximation in this study with results previously published for homogeneous, regularly shaped, breast Monte Carlo simulations for the three modalities/techniques studied.

	Mammography	BCT 49 kVp	BCT 80 kVp
This study	0.18 (0.13–0.35)	0.46 (0.41–0.55)	0.89 (0.83–0.93)
Comparison study	0.19 (0.11–0.39)	0.50 (0.46–0.56)	0.84–0.90
Source	Tables 2, 3, and 6 in Ref. 54	Table 1 in Ref. 17	Fig. 13(b) in Ref. 16

results are based on 20 cases, while all mammography results are based on 19 cases.

Table I provides summarized data of the characteristics of the breasts included in this study. As can be seen, the glandular density distribution, estimated from both the uncompressed and compressed versions of the breasts, follows the characteristics described by Yaffe *et al.*, who found that the glandular density of an average breast is approximately 15%–20% and that most breasts are included in the range of 5%–50%.[19]

III.C. Comparison to previous studies

Table II shows the results of the comparison of the normalized glandular dose estimates for the homogeneous breast tissue mixture approximation to previously published studies. As can be seen, considering the variations in breast shapes between the *in vivo* based breasts studied here and the regular phantoms used in the comparison studies, the values show excellent concordance.

III.D. Heterogeneous vs homogeneous mean normalized glandular dose comparison

The use of the homogeneous breast tissue mixture approximation overestimates the mean glandular dose by a mean factor of 1.27 (range: 0.84–2.17) for mammography, 1.08 (range: 0.94–1.23) for BCT with a 49 kVp spectrum and 1.04 (range: 1.00–1.09) for BCT with an 80 kVp spectrum. For all three modalities/techniques the difference between the dose estimates was statistically significant. Figure 4 shows a graph of the normalized mean glandular dose for the homogeneous

breast tissue mixture as a function of that of the breasts with the actual heterogeneous tissue distribution, for the mammography acquisitions and the 49 kVp and 80 kVp BCT acquisitions. Also included in the graph is the identity line.

As can be seen, the homogeneous approximation results in a higher mean glandular dose than the heterogeneous estimate for all breasts in all three modalities/techniques except for two breasts undergoing mammography and two breasts undergoing BCT with a tube voltage of 49 kVp. The result of the statistical tests on the differences between the dose estimates is shown in Table III.

Figure 5 shows a box-whisker plot of the ratio of the homogeneous mean glandular dose divided by the heterogeneous estimate for each modality/technique. It can be clearly seen that the overestimation of the glandular dose is most severe for mammography, and that for BCT it is lower for the 80 kVp spectrum compared to the 49 kVp. Figure 6 shows this ratio as a function of each breast's volumetric glandular density. Unfortunately, due to the relatively low number of cases included in this study, any trend in this ratio with relation to glandular density is not apparent.

Figure 7 shows coronal slices of the heterogeneous and homogeneous tissue distributions of one of the breasts studied with the dose deposition superimposed. The values for the dose deposition scale are normalized glandular dose in mGy per mGy air kerma. The case shown here is one for which the normalized glandular dose ratio between the two breast tissue definitions is similar to the mean of the ratios for all three modalities, so it was selected as representative of an average case. As expected,[17,51,55] these dose maps clearly show, especially for mammography and the lower energy BCT
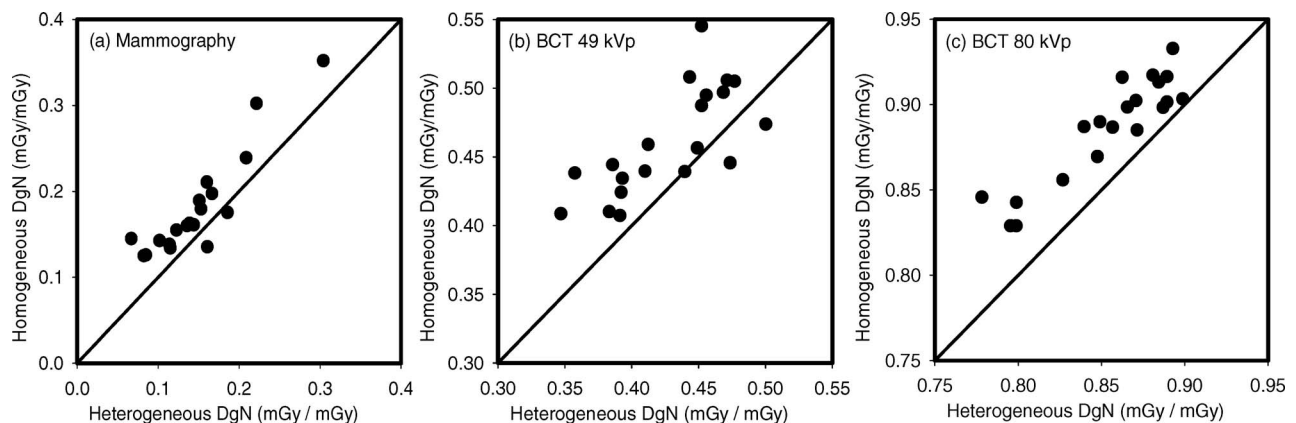

FIG. 4. Comparison of the estimated normalized mean glandular dose for the homogeneous tissue mixture approximation to the estimate based on the true glandular tissue distribution for the (a) mammography, (b) 49 kVp BCT, and (c) 80 kVp BCT acquisitions. The diagonal line is the identity line.

TABLE III. Results of the Wilcoxon Signed Ranks test on the normalized glandular dose estimates for the homogeneous tissue mixture approximation and the true heterogeneous tissue distribution.

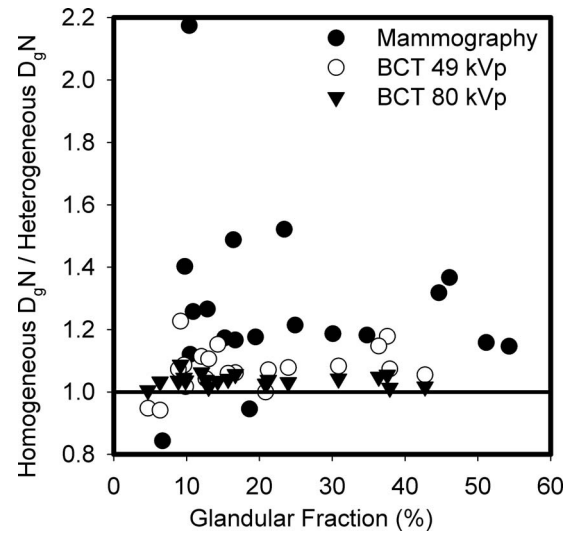|	Mammography	BCT 49 kVp	BCT 80 kVp
n	19	20	20
Wilcoxon's W	−174	−188	−210
Z	−3.501	−3.509	−3.920
p	0.000463	0.000449	0.0000886

FIG. 6. Ratio of homogeneous to heterogeneous D_gN for each modality/technique as a function of breast volumetric glandular density. Given the limited number of cases it is difficult to identify a pattern for this relationship, if one exists.

acquisition, the preferential dose deposition in the tissue closer to the x-ray source position of the breast. Therefore, since the glandular tissue tends to be centrally located in the breast, the homogeneous tissue mixture approximation results in an overestimation of the glandular dose compared to when using the true heterogeneous distribution. For the 80 kVp BCT acquisition, the dose deposition is more homogeneous, resulting in a small overestimation.

IV. DISCUSSION

As first hinted at by Dance *et al.*,[30] the use of the homogeneous tissue mixture approximation does result in an overestimation of the normalized mean glandular dose to actual patients' breasts. As could be expected, this overestimation is higher for mammography than for BCT, since the former uses lower energy x-rays than the latter. In fact, for some applications, the overestimation in BCT, although statistically significant may not be clinically so.

Given that in actual patients' breasts the glandular tissue tends to be more concentrated in the center of the breast, the homogeneous approximation overestimates how much glandular tissue is close to the perimeter of the breast since it spreads the total glandular tissue content evenly throughout the entire breast tissue volume. Therefore, for imaging conditions with x rays of lower penetrability the difference between the two dose estimates is increased. It has been shown that the energy deposition throughout the whole breast volume is more homogeneous in BCT than in mammography,[17] and that

this homogeneity increases with increasing x-ray energy,[55] which corresponds with the results obtained here.

As shown in Sec. III, a single breast undergoing mammography resulted in a normalized glandular dose for the homogeneous tissue mixture approximation of 2.17 times that of the heterogeneous distribution, representing a clear outlier in this limited data set. From qualitative evaluation of the tissue distribution of this breast, it was found that most of the glandular tissue is distributed in two main locations: mostly towards the center the breast and at one side of the breast, which under compression was located towards the bottom of the breast, furthest away from the x-ray source. It is expected that if a large portion of the glandular tissue in the breast is situated at the bottom of the breast, this would introduce an important deviation in the glandular dose estimate when approximating the glandular distribution as homogeneous about the entire breast.
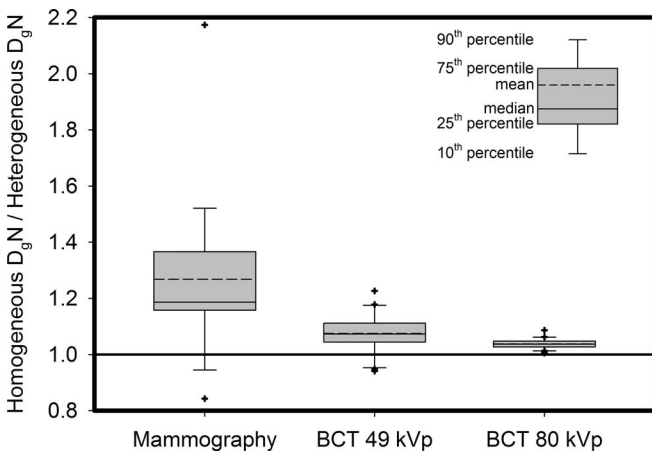

FIG. 5. Box-whisker plot of the ratios of homogeneous to heterogeneous D_gN for each modality/technique. The legend in the top right identifies the meaning of each component of the plot. The symbols denote outliers.
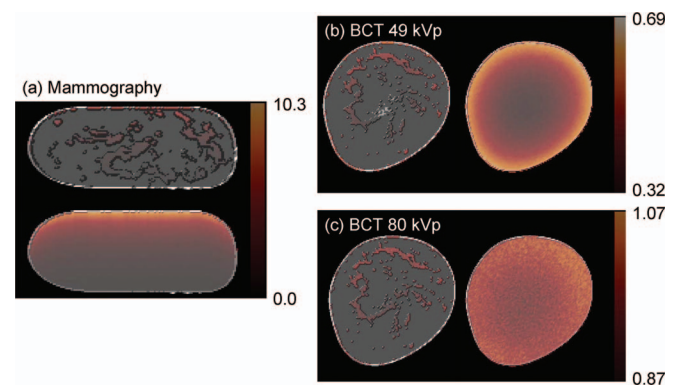

FIG. 7. Coronal slice of the dose depositions superimposed on the tissue distribution for a representative case for (a) mammography (top: heterogeneous, bottom: homogeneous) and BCT at (b) 49 kVp and (c) 80 kVp (right: homogeneous, left: heterogeneous). As expected, for the heterogeneous breast, glandular dose is only deposited in the glandular voxels, so the adipose voxels contain no dose deposition. The values of the scales are normalized glandular dose in mGy per mGy air kerma.

A comparison of the ratios of the normalized glandular dose obtained from the heterogeneous and homogenous compositions for the three modalities/techniques studied shows that even for comparative studies the use of the homogeneous approximation can be problematic. For example, a study comparing mammography to BCT performed with a tube voltage of 80 kVp using the homogeneous breast tissue approximation would be comparing mammography dose values which are overestimated, on average, 27% to BCT dose values which are, on average, only 4% overestimated. For the 19 patient breasts included in this study for which results for both modalities are available, the ratio of the 80 kVp BCT overestimation to that of the mammography overestimation on a case-by-case basis varies from 0.50 to 1.23 (mean = 0.85). For mammography vs the 49 kVp BCT, this range of ratios is 0.56–1.12 (mean = 0.88). Finally, this range of ratios between the two BCT techniques is 0.89–1.10 (mean = 0.97). Clearly, the use of the homogeneous breast model can introduce a considerable error in dose comparisons when the two modalities compared differ considerably in characteristics such as the x-ray energy. For comparison studies between modalities/techniques that are more similar, e.g., BCT with a tube voltage of 49 kVp vs 80 kVp, the errors introduced are smaller. The third spectrum being used in BCT studies, with a tube voltage of 60 kVp and a Ce filter,[50] has a beam quality intermediate between the two studied here, so the results for that spectrum could be expected to also fall in between the two obtained in this study.

The present study is limited mainly by the low number of cases studied. To better characterize how the homogeneous breast tissue mixture approximation overestimates glandular dose under different acquisition conditions, and especially for breasts of different characteristics, a much larger sample size is required. With a sufficient number of cases, it could be possible to develop correction factors by which these homogeneous approximation estimates could be corrected to provide better dose estimates in absolute terms.

Another limitation of this study is the possible mismatch between the compressed tissue simulated as being in the field of view during the mammography acquisition and that actually imaged during an actual mammogram. However, since the dose estimate comparison is made in a paired fashion to the equivalent volume, this should not have a major impact on the results. In addition, this study simulated only the CC view mammographic acquisition, ignoring the medio-lateral oblique (MLO) view. However, since the breast data are obtained from BCT images in which the breast is not compressed, it is most probable that breast tissue in the axillary tail and pectoralis muscle tissue that would be included in the MLO field of view does not appear in our compressed breast simulations, making a realistic simulation of the MLO view with this BCT data impossible.

V. CONCLUSIONS

This study with a limited number of cases found that the approximation of defining the breast as a homogeneous mixture of adipose and glandular tissue surrounded by skin re-

sults in a significant overestimate of the mean glandular dose. As expected, the overestimate is largest for the lowest energy modality, mammography, with the overestimate being small for imaging with relatively high x-ray energies. Since estimates of this dose measure are used in absolute terms to estimate increased risk for cancer development it is clear that a thorough understanding of this overestimate is needed, and, if possible, correction factors or new metrics should be developed to better reflect the actual mean glandular dose consequences of x-ray based breast imaging modalities such as mammography, tomosynthesis, and dedicated breast CT. In addition, it was found that comparative studies that include two modalities or techniques of very different characteristics can also be problematic when using the homogeneous tissue mixture approximation.

a)Author to whom correspondence should be addressed. Electronic mail: E-mail: isechop@emory.edu; Telephone: (404)712-2412; Fax: (404)712-5813.

[1]J. Ewton, R. Shalek, and R. Egan, "Estimated radiation dose during mammography," Cancer Bull. **14**, 116–117 (1962).

[2]G. R. Hammerstein, D. W. Miller, D. R. White, M. E. Masterson, H. Q. Woodard, and J. S. Laughlin, "Absorbed radiation dose in mammography," Radiology **130**, 485–491 (1979).

[3]D. R. Dance, "The Monte Carlo calculation of integral radiation dose in xeromammography," Phys. Med. Biol. **25**, 25–37 (1980).

[4]K. Doi and H. P. Chan, "Evaluation of absorbed dose in mammography: Monte Carlo simulation studies," Radiology **135**, 199–208 (1980).

[5]D. R. Dance, "Monte Carlo calculation of conversion factors for the estimation of mean glandular breast dose," Phys. Med. Biol. **35**, 1211–1219 (1990).

[6]X. Wu, G. T. Barnes, and D. M. Tucker, "Spectral dependence of glandular tissue dose in screen-film mammography," Radiology **179**, 143–148 (1991).

[7]X. Wu, E. L. Gingold, G. T. Barnes, and D. M. Tucker, "Normalized average glandular dose in molybdenum target-rhodium filter and rhodium target-rhodium filter mammography," Radiology **193**, 83–89 (1994).

[8]J. M. Boone, "Glandular breast dose for monoenergetic and high-energy x-ray beams: Monte Carlo assessment," Radiology **213**, 23–37 (1999).

[9]D. R. Dance, C. L. Skinner, and G. Alm Carlsson, "Breast dosimetry," Appl. Radiat. Isot. **50**, 185–203 (1999).

[10]D. R. Dance, A. K. Thilander, M. Sandborg, C. L. Skinner, I. A. Castellano, and G. A. Carlsson, "Influence of anode/filter material and tube potential on contrast, signal-to-noise ratio and average absorbed dose in mammography: A Monte Carlo study," Br. J. Radiol. **73**, 1056–1067 (2000).

[11]J. M. Boone, "Normalized glandular dose (DgN) coefficients for arbitrary x-ray spectra in mammography: Computer-fit values of Monte Carlo derived data," Med. Phys. **29**, 869–875 (2002).

[12]D. R. Dance, K. C. Young, and R. E. van Engen, "Estimation of mean glandular dose for breast tomosynthesis: Factors for use with the UK, European and IAEA breast dosimetry protocols," Phys. Med. Biol. **56**, 453–471 (2011).

[13]A. K. W. Ma, D. G. Darambara, A. Stewart, S. Gunn, and E. Bullard, "Mean glandular dose estimation using MCNPX for a digital breast tomosynthesis system with tungsten/aluminum and tungsten/aluminum + silver x-ray anode-filter combinations," Med. Phys. **35**, 5278–5289 (2008).

[14] I. Sechopoulos and C. J. D'Orsi, "Glandular radiation dose in tomosynthesis of the breast using tungsten targets," J. Appl. Clin. Med. Phys. 9, 161–171 (2008).

[15] I. Sechopoulos, S. Suryanarayanan, S. Vedantham, C. D'Orsi, and A. Karellas, "Computation of the glandular radiation dose in digital tomosynthesis of the breast," Med. Phys. 34, 221–232 (2007).

[16] J. M. Boone, N. Shah, and T. R. Nelson, "A comprehensive analysis of DgN(CT) coefficients for pendant-geometry cone-beam breast computed tomography," Med. Phys. 31, 226–235 (2004).

[17] I. Sechopoulos, S. S. J. Feng, and C. J. D'Orsi, "Dosimetric characterization of a dedicated breast computed tomography clinical prototype," Med. Phys. 37, 4110–4120 (2010).

[18] S. Vedantham, L. Shi, A. Karellas, and F. Noo, "Dedicated breast CT: Radiation dose for circle-plus-line trajectory," Med. Phys. 39, 1530–1541 (2012).

[19] M. J. Yaffe, J. M. Boone, N. Packard, O. Alonzo-Proulx, S. Y. Huang, C. L. Peressotti, A. Al-Mayah, and K. Brock, "The myth of the 50-50 breast," Med. Phys. 36, 5437–5443 (2009).

[20] S.-Y. Huang, J. M. Boone, K. Yang, A. L. C. Kwan, and N. J. Packard, "The effect of skin thickness determined using breast CT on mammographic dosimetry," Med. Phys. 35, 1199–1206 (2008).

[21] R. E. Hendrick, E. D. Pisano, A. Averbukh, C. Moran, E. A. Berns, M. J. Yaffe, B. Herman, S. Acharyya, and C. Gatsonis, "Comparison of acquisition parameters and breast dose in digital mammography and screen-film mammography in the American College of Radiology Imaging Network Digital Mammographic Imaging Screening Trial," Am. J. Roentgenol. 194, 362–369 (2010).

[22] D. C. Spelic, "Updated trends in mammography dose and image quality," 2010 (Available from: http://www.fda.gov/Radiation-EmittingProducts/MammographyQualityStandardsActandProgram/FacilityScorecard/ucm113352.htm. Last accessed March 7, 2012).

[23] K. C. Young, A. Burch, and J. M. Oduko, "Radiation doses received in the UK breast screening programme in 2001 and 2002," Br. J. Radiol. 78, 207–218 (2005).

[24] M. J. Yaffe and J. G. Mainprize, "Risk of radiation-induced breast cancer from mammographic screening," Radiology 258, 98–105 (2011).

[25] A. Berrington de Gonzalez, C. D. Berg, K. Visvanathan, and M. Robson, "Estimated risk of radiation-induced breast cancer from mammographic screening for young BRCA mutation carriers," J. Natl. Cancer Inst. 101, 205–209 (2009).

[26] A. Berrington de Gonzalez and G. Reeves, "Mammographic screening before age 50 years in the UK: Comparison of the radiation risks with the mortality benefits," Br. J. Cancer 93, 590–596 (2005).

[27] R. E. Hendrick, "Radiation doses and cancer risks from breast imaging studies," Radiology 257, 246–253 (2010).

[28] E. Warner, "Breast-cancer screening," N. Engl. J. Med. 365, 1025–1032 (2011).

[29] Y. Yi, C.-J. Lai, T. Han, Y. Zhong, Y. Shen, X. Liu, S. Ge, Z. You, T. Wang, and C. C. Shaw, "Radiation doses in cone-beam breast computed tomography: A Monte Carlo simulation study," Med. Phys. 38, 589–597 (2011).

[30] D. R. Dance, R. A. Hunt, P. R. Bakic, A. D. A. Maidment, M. Sandborg, G. Ullman, and G. Alm Carlsson, "Breast dosimetry using high-resolution voxel phantoms," Radiat. Prot. Dosim. 114, 359–363 (2005).

[31] R. Ning, D. Conover, Y. Yu, Y. Zhang, W. Cai, R. Betancourt-Benitez, and X. Lu, "A novel cone beam breast CT scanner: System evaluation," Proc. SPIE 6510, 651030–651039 (2007).

[32] R. Betancourt-Benitez, R. Ning, D. Conover, and S. Liu, "NPS characterization and evaluation of a cone beam CT breast imaging system," J. X-Ray Sci. Technol. 17, 17–40 (2009).

[33] R. Betancourt-Benitez, R. Ning, D. Conover, and S. Liu, "Composite modulation transfer function evaluation of a cone beam computed tomography breast imaging system," Opt. Eng. 48, 117002–117011 (2009).

[34] A. O'Connell, D. L. Conover, Y. Zhang, P. Seifert, W. Logan-Young, C.-F. L. Lin, L. Sahler, and R. Ning, "Cone-beam CT for breast imaging: Radiation dose, breast coverage, and image quality," Am. J. Roentgenol. 195, 496–509 (2010).

[35] L. A. Feldkamp, L. C. Davis, and J. W. Kress, "Practical cone-beam algorithm," J. Opt. Soc. Am. A 1, 612–619 (1984).

[36] X. Yang, I. Sechopoulos, and B. Fei, "Automatic tissue classification for high-resolution breast CT images based on bilateral filtering," Proc. SPIE 7962, 79623H (2011).

[37] R. Bhagtani and T. G. Schmidt, "Simulated scatter performance of an inverse-geometry dedicated breast CT system," Med. Phys. 36, 788–796 (2009).

[38] A. L. C. Kwan, J. M. Boone, and N. Shah, "Evaluation of x-ray scatter properties in a dedicated cone-beam breast CT scanner," Med. Phys. 32, 2967–2975 (2005).

[39] B. Liu, S. J. Glick, and C. Groiselle, "Characterization of scatter radiation in cone beam CT mammography," Proc. SPIE 5745, 818–827 (2005).

[40] P. M. Shikhaliev, "Beam hardening artefacts in computed tomography with photon counting, charge integrating and energy weighting detectors: A simulation study," Phys. Med. Biol. 50, 5813–5827 (2005).

[41] C. Tomasi and R. Manduchi, "Bilateral filtering for gray and color images," in *Proceedings of the Sixth International Conference on Computer Vision* (IEEE, New Delhi, India, 1998), pp. 839–846.

[42] C. Zyganitidis, K. Bliznakova, and N. Pallikarakis, "A novel simulation algorithm for soft tissue compression," Med. Biol. Eng. Comput. 45, 661–669 (2007).

[43] A. L. Kellner, T. R. Nelson, L. I. Cervino, and J. M. Boone, "Simulation of mechanical compression of breast tissue," IEEE Trans. Biomed. Eng. 54, 1885–1891 (2007).

[44] I. Sechopoulos, S. Suryanarayanan, S. Vedantham, C. J. D'Orsi, and A. Karellas, "Scatter radiation in digital tomosynthesis of the breast," Med. Phys. 34, 564–576 (2007).

[45] S. Agostinelli *et al.*, "Geant4: A simulation toolkit," Nucl. Instrum. Methods Phys. Res. A 506, 250–303 (2003).

[46] J. Allison *et al.*, "Geant4 developments and applications," IEEE Trans. Nucl. Sci. 53, 270–278 (2006).

[47] J. M. Boone, T. R. Fewell, and R. J. Jennings, "Molybdenum, rhodium, and tungsten anode spectral models using interpolating polynomials with application to mammography," Med. Phys. 24, 1863–1874 (1997).

[48] K. Cranley, B. J. Gilmore, G. W. A. Fogarty, and L. Desponds, "Catalogue of diagnostic x-ray spectra and other data," Report No. 78 (Institute of Physics and Engineering in Medicine, York, 1997).

[49] K. K. Lindfors, J. M. Boone, T. R. Nelson, K. Yang, A. L. C. Kwan, and D. F. Miller, "Dedicated breast CT: Initial clinical experience," Radiology 246, 725–733 (2008).

[50] P. Madhav, D. J. Crotty, R. L. McKinley, and M. P. Tornai, "Evaluation of tilted cone-beam CT orbits in the development of a dedicated hybrid mammotomograph," Phys. Med. Biol. 54, 3659–3676 (2009).

[51] D. J. Crotty, S. L. Brady, D. V. C. Jackson, G. I. Toncheva, C. E. Anderson, T. T. Yoshizumi, and M. P. Tornai, "Investigating the dose distribution in the uncompressed breast with a dedicated CT mammotomography system," Proc. SPIE 7622, 762229–762212 (2010).

[52] J. Sempau, A. Sánchez-Reyes, F. Salvat, H. O. b. Tahar, S. B. Jiang, and J. M. Fernández-Varea, "Monte Carlo simulation of electron beams from an accelerator head using PENELOPE," Phys. Med. Biol. 46, 1163–1186 (2001).

[53] L. Wilkinson and J. C. P. Heggie, "Glandular breast dose: Potential errors [eletter]," Radiology, 2000 (Available URL: http://radiology.rsna.org/content/213/1/23/reply#radiology_el_5. Last accessed November 21, 2005).

[54] D. R. Dance, C. L. Skinner, K. C. Young, J. R. Beckett, and C. J. Kotre, "Additional factors for the estimation of mean glandular breast dose using the UK mammography dosimetry protocol," Phys. Med. Biol. 45, 3225–3240 (2000).

[55] S. C. Thacker and S. J. Glick, "Normalized glandular dose (DgN) coefficients for flat-panel CT breast imaging," Phys. Med. Biol. 49, 5433–5444 (2004).

[56] http://www-unix.mcs.anl.gov/mpi/mpich2/.